International Journal of Chemistry and Pharmaceutical Sciences
ISSN: 2321-3132 | CODEN (USA): IJCPNH | Publisher: Pharma Research Library
Journal Home Page: http://www.pharmaresearchlibrary.com/ijcps
DOI: https://doi.org/10.30904/j.ijcps.2024.4776
Int. J. of Chem. Pharm. Sci., 12(1), 2024: 43-47

Designing Characterization and Bioaccumulation of Nanomaterials for Degradation of Environmental Pollutants

Sanjay Rajamgari[1]*, Hrushikesh Mahanty[2], Praveen Kumar N[3]
[1]Master Trainer/Support Engineer, Environmental Impact Assessment (EIA) Division, SEIAA, A3, Industrial Estate, Sanathnagar, Hyderabad, Telangana - 500 018.
[2]Master Trainer/Support Engineer, Environmental Impact Assessment (EIA) Division, SEIAA, 5RF 2/1, Unit-9, Bhubaneswar, Odisha- 751022.
[3]Master trainer/Supporting Engineer, Environmental Impact Assessment (EIA) Division, SEIAA, 4th floor, Dempo tower, Patto, Panjim, Goa-403001

Abstract
Environmental pollution, particularly from dyes and pigments, degrades water quality and poses health risks. Conventional water treatment systems often fail to address localized dye contamination, necessitating advanced decentralized solutions. This study explores the synthesis and characterization of six novel molybdenum and tin-based nanomaterials like MoO_3, MoS_2, and SnS_2 nanoparticles, along with their core-shell nanocomposites incorporating $CoMnFe_2O_4$ designed for efficient dye degradation under visible LED light. The nanomaterials were synthesized using the hydrothermal method and characterized through Raman Spectroscopy, FTIR, HRTEM, XRD, and UV-DRS. Structural analysis confirmed varied morphologies and crystallite sizes ranging from 4 to 32 nm. Optical band gap measurements indicated enhanced photocatalytic properties, attributed to oxygen vacancies and intercalation effects. These specific nanocomposites, highlight their potential as effective, eco-friendly photocatalysts for environmental pollutant removal.
Keywords: nanomaterials, environmental pollutants, molybdenum, tin-based.

Citation: *Sanjay Rajamgari, et al. Designing Characterization and Bioaccumulation of Nanomaterials for Degradation of Environmental Pollutants, Int. J. of Chem. and Pharm. Sci., 12(1), 2024: 43-47.*

Contents:

***Corresponding author**
Sanjay Rajamgari
Master Trainer/Support Engineer,
Environmental Impact Assessment (EIA) Division,
SEIAA, A3, Industrial Estate, Sanathnagar, Hyderabad, T.G

Article History:
Received : 25 Sept 2024
Revised : 29 Oct 2024
Accepted : 05 Dec 2024
Published : 20 Dec 2024

1. Introduction

Water pollution is a major global threat, causing 3.1% of deaths worldwide (WHO, 2002). Rapid population growth, industrialization, and waste discharge exacerbate water contamination, reducing safe drinking water availability (Chong et al., 2010). Over 780 million people lack access to clean water, a number expected to rise (WHO, 2012). Surface and groundwater are polluted by chemicals, heavy metals, and organic compounds, with dyes from textile industries being major contaminants (Gupta et al., 2013). These dyes obstruct sunlight, harm aquatic life, and pose carcinogenic and mutagenic risks (Ahmad et al., 2015).

Microbial contamination further depletes dissolved oxygen (DO), causing disease outbreaks responsible for over 2.2 million deaths annually (WHO, 2018). Waterborne infections, membrane fouling in treatment plants, and increased operational costs remain critical challenges (Chellam & Cogan, 2011).

Nanotechnology offers efficient water purification solutions. Nano-photocatalysts, using light to degrade pollutants, generate reactive oxygen species (ROS) that break down organic toxins (Akyol & Bayramoglu, 2008). Metal oxides like ZnO, TiO_2, and MoO_3 have shown promise in advanced oxidation processes (Chakrabarti & Dutta, 2004). However, concerns over nanomaterial toxicity, bioaccumulation, and environmental impact persist. Nanoparticles can disrupt plant physiology,

affecting seed germination, growth, and metabolic processes (Siddiqi & Husen, 2016). Bioaccumulation risks in the food chain further highlight the need for sustainable nanomaterial design (Grieger et al., 2009). This study focuses on the synthesis, characterization, and application of MoO_3, MoS_2, and SnS_2 nanomaterials for dye degradation and antibacterial properties. Their effects on rice plants were also assessed under controlled conditions. By leveraging visible-light-driven nanocatalysts, this research aims to advance eco-friendly solutions for water purification while evaluating potential ecological risks. Different types of dyes in the environment:

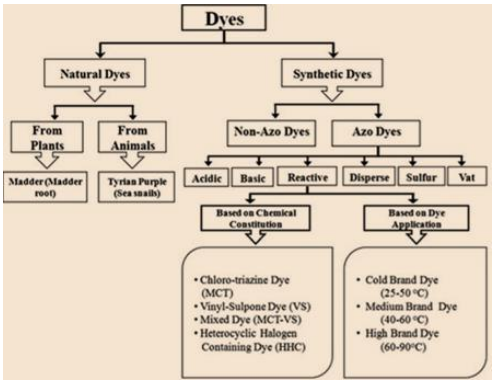

Fig.1. Different types of dyes in the environment

2. Materials and methods

Materials required

All chemicals used in this study were analytical grade and used without further purification. Methylene blue ($C_{16}H_{18}N_3SCl$), Methyl orange ($C_{14}H_{14}N_3O_3NaS$), Malachite green ($C_{23}H_{25}N_2$), Eosin yellow ($C_{20}H_6O_5Br_4Na_2$), Rhodamine B (C28H31ClN2O3), Eriochrome black T ($C_{20}H_{12}N_3O_7SNa$), Amido black 10B ($C_{22}H_{14}N_6Na_2O_9S_2$) was purchased from Sigma-Aldrich (USA). All aqueous solutions were prepared with Milli-Q water (≥ 18.2 Mcm).

Photocatalytic study of nanomaterials

The photocatalytic activity of synthesized MoO_3 were evaluated by studying the degradation of cationic i.e. methylene blue (MB), malachite green (MG), rhodamine B (RhB) and anionic i.e. eosin yellow (EY), methyl orange (MO), eriochrome black T (EBT), amido black 10B (AB) dyes as model pollutants. The experimental setup for the photocatalytic degradation of dye is illustrated as fig. 2. The photodegradation reactions were performed under visible light (λ ≥ 400 nm) using white LED light (12W, WLED; 400-700nm) in two independent experimental setups as follows: (i) Fixed concentration (0.1 g/l) of nanomaterial was suspended in 30 ml solution of varying concentrations (0-50 mg/l) containing either cationic or anionic dyes (ii) Varying concentrations (0.01 to 0.1 g/l) of nanomaterial were suspended in a 30 ml aqueous solution having fixed quantity (10 mg/l) cationic or anionic dyes. Prior to exposure to visible light, the mixture of dye and nanomaterials were stirred vigorously at room temperature for 30 min in dark so as to achieve adsorption–desorption equilibrium on the photocatalyst surface remained uniform across all experiments. The solution was then exposed to visible light under continuous stirring. Dye degradation was monitored by extracting 1 ml aliquots at 15-minute intervals over a total reaction time of 90 minutes. Changes in dye absorption were analyzed using a UV-Vis spectrophotometer (Genesys 10uv, Thermo-Fischer, USA). Similar experiments were conducted with MoS_2, SnS_2, $CoMnFe_2O_4@MoO_3$, $CoMnFe_2O_4@MoS_2$, and $CoMnFe_2O_4@SnS_2$ nanomaterials. Dye solutions of varying concentrations (1 ppm, 5 ppm, 10 ppm, and 20 ppm) were prepared. The concentration ratio (C/C_0) was measured at specific wavelengths for different dyes: 662 nm for MB, 621 nm for MG, 553 nm for RhB, 612 nm for EY, 464 nm for MO, 573 nm for EBT, and 619 nm for AB, where C_0 is the initial concentration, and C is the concentration at time t. Additionally, degradation efficiency (%) and reaction kinetics of nanoparticle-catalyzed reactions were evaluated.

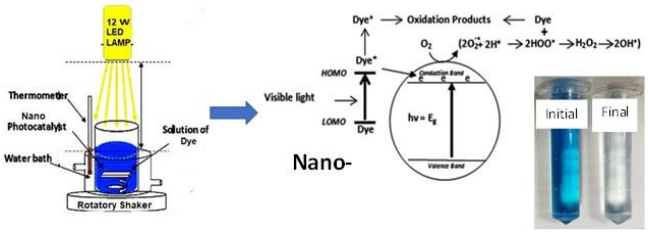

Fig. 2. Schematic representation of the experimental setup in laboratory for studying photocatalytic degradation of dyes under visible light

3. Results and discussion

An understanding of dye degradation and how it is influenced by different parameters is important for the design and optimization of an industrial system. The photocatalytic degradation depends on several factors including concentration of dye, dose of nanomaterials, type of dyes and duration of exposure.

Photocatalytic Studies of MoO_3, $CoMnFe_2O_4@MoO_3$ Nanomaterials: The photocatalytic performance of MoO_3 nanoparticles and $CoMnFe_2O_4@MoO_3$ Nano composites was studied under visible light (λ ≥ 400 nm) using cationic and anionic dyes. UV-Vis absorption spectra confirmed no significant changes in pure dye solutions under LED light. Fig. 3 (a, b) presents removal efficiency vs. time for MoO_3 (0.01–0.1 g/L) and $CoMnFe_2O_4@MoO_3$ (0.2–1 g/L) with 10 mg/L MB dye over 90 min. Higher MoO_3 concentrations increased removal efficiency, peaking at 96% in 15 min with 0.1 g/L. $CoMnFe_2O_4@MoO_3$ showed 73% efficiency at 1 g/L, indicating $CoMnFe_2O_4$'s limited photocatalytic role. The final removal after 90 min was 99% for both materials. Efficiency reductions were attributed to turbidity, agglomeration, and catalyst deactivation. Photocatalysis follows electron–hole pair formation in MoO_3, generating hydroxyl ($OH^{\cdot}$) and superoxide ($O_2^{\cdot -}$) radicals that degrade MB. Increased photonic efficiency enhances degradation via repeated $OH^{\cdot}$ attacks. The removal of different dye concentrations (Fig. 3 c, d) shows 96% degradation of 10 mg/L MB in 15 min for MoO_3, with reduced efficiency at higher dye concentrations due to the blanket effect. Fig. 3 (e, f) indicates MoO_3 nanoparticles are more effective for cationic dyes, except EY, with 99% MB removal.

$CoMnFe_2O_4$@MoO_3 nanocomposites showed lower efficiencies, particularly for RhB and anionic dyes.

Photocatalytic Studies of MoS_2 and $CoMnFe_2O_4$ @MoS_2 Nanomaterials:

The photocatalytic activity of MoS_2 and $CoMnFe_2O_4$@MoS_2 was evaluated under visible light. Fig. 4 (a, b) shows removal efficiency for MoS_2 (0.1–0.8 g/L) and $CoMnFe_2O_4$@MoS_2 (0.08–0.8 g/L) with 10 mg/L MB. MoS_2 exhibited higher dark-period adsorption (27% at 0.1g/L) than $CoMnFe_2O_4$ @MoS_2 (10% at 0.08 g/L) due to its nanoflower-like structure. Photodegradation was fastest in the first 15 min, with MoS_2 achieving 88% removal at 0.8 g/L, while $CoMnFe_2O_4$@MoS_2 reached 47%. After 90 min, MoS_2 showed ≥96% degradation at ≥0.2 g/L, whereas $CoMnFe_2O_4$@MoS_2 reached only 72% at ≥0.4 g/L. Dye concentration effects (Fig. 4 c, d) showed MoS_2 removing 98% of 10 mg/L MB, decreasing with higher dye concentrations due to the blanket effect. $CoMnFe_2O_4$ @MoS_2 exhibited lower efficiency (42% at 2 mg/L, 13% at 10 mg/L). Fig. 4 (e, f) highlights MoS_2's superior performance for cationic dyes (97–99%), with lower removal of anionic dyes. $CoMnFe_2O_4$@MoS_2 had reduced efficiency, particularly for EY and MO.

Photocatalytic Studies of SnS_2 and $CoMnFe_2O_4$ @SnS_2 Nanomaterials: SnS_2 and $CoMnFe_2O_4$@SnS_2 were analyzed under visible light. Fig. 5 (a, b) shows removal efficiency for SnS_2 (0.2–1 g/L) and $CoMnFe_2O_4$@SnS_2 (0.2–2 g/L) with 10 mg/L MB. SnS_2 exhibited higher adsorption (23% at 0.2 g/L) than $CoMnFe_2O_4$@SnS_2 (6% at 0.2 g/L). After light exposure, 1 g/L SnS_2 degraded 93% of MB in 15 min, while 2 g/L $CoMnFe_2O_4$@SnS_2 achieved only 40%. After 90 min, SnS_2 removed ≥91% of MB at ≥0.4 g/L, while $CoMnFe_2O_4$@SnS_2 peaked at 82%. Dye concentration studies (Fig. 5 c, d) showed SnS_2 degrading 97% of 10 mg/L MB, decreasing with increasing dye concentration. $CoMnFe_2O_4$@SnS_2 had lower removal (95% at 2 mg/L, 65% at 10 mg/L). Fig. 5 (e, f) shows SnS_2 effectively removing cationic dyes (91–97%) and anionic dyes at lower rates. $CoMnFe_2O_4$@SnS_2 was less efficient overall.

Kinetics of Dye Degradation:

The MB degradation kinetics were analyzed using the Langmuir–Hinshelwood model. MoO_3, MoS_2, and SnS_2 nanoparticles exhibited superior photocatalytic efficiency compared to their respective $CoMnFe_2O_4$-based nanocomposites are shown in fig. 6.

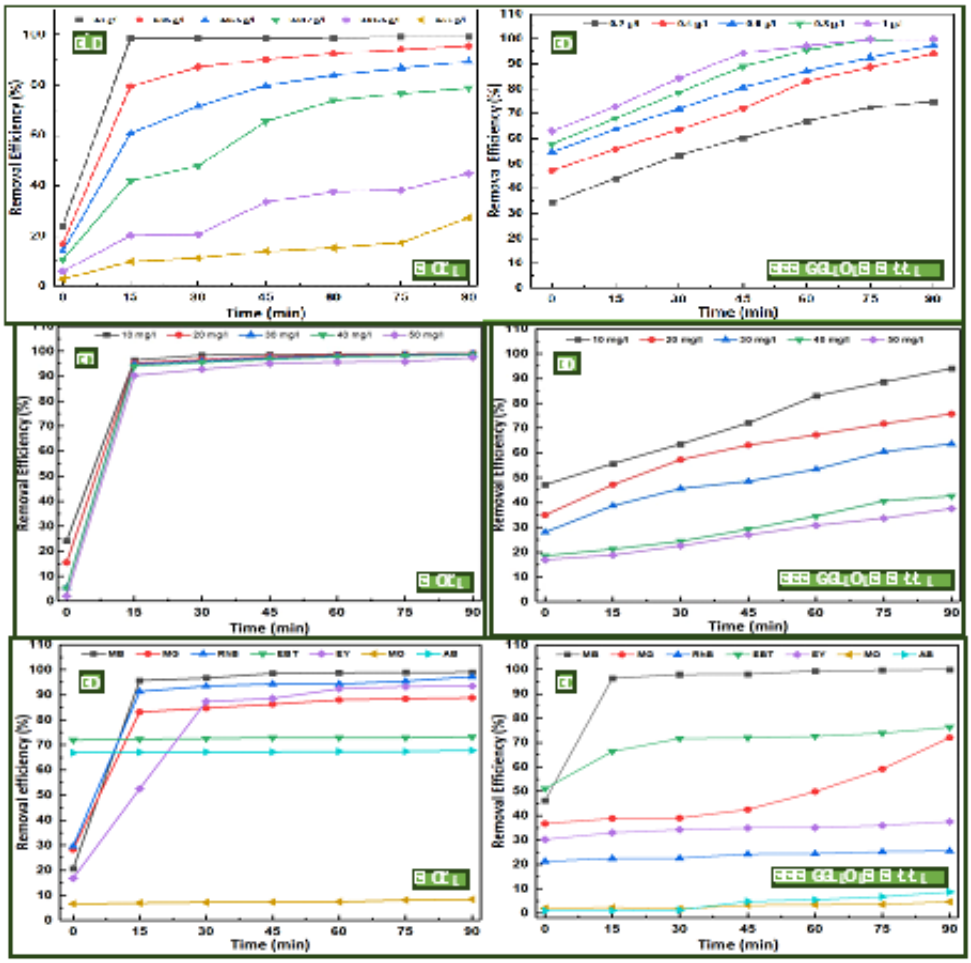

Fig. 3. Photocatalytic dye degradation of dyes in presence of (a), (c), (e) MoO3 and (b), (d), (f) CoMnFe2O4@MoO3 under following reaction conditions: (a), (b) varying concentration (0.01 g/l-0.1g/l) of nanomaterial in presence of 10 mg/l MB dye; (c), (d) varying concentration (10 mg/l-50 mg/l) of MB dye in presence of 0.1 g/l of nanomaterial, and (e), (f) in presence of different dyes at 10mg/l concentration and 0.1 g/l of nanomaterial.

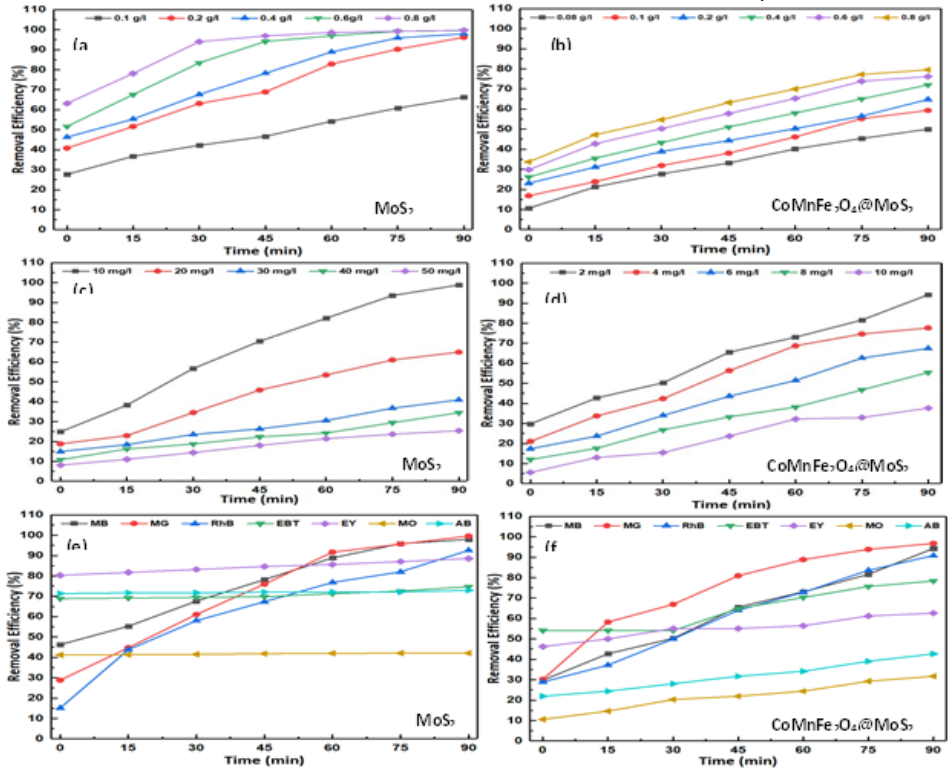

Fig. 4 Photocatalytic dye degradation of dyes in presence of (a), (c), (e) MoS2 and (b), (d), (f) CoMnFe2O4@MoS2 under following reaction conditions: (a), (b) varying concentration (0.01 g/l-0.1g/l) of nanomaterial in presence of 10 mg/l MB dye; (c), (d) varying concentration (10 mg/l-50 mg/l) of MB dye in presence of 0.1 g/l of nanomaterial, and (e), (f) in presence of different dyes at 10mg/l concentration and 0.1 g/l of nanomaterial.

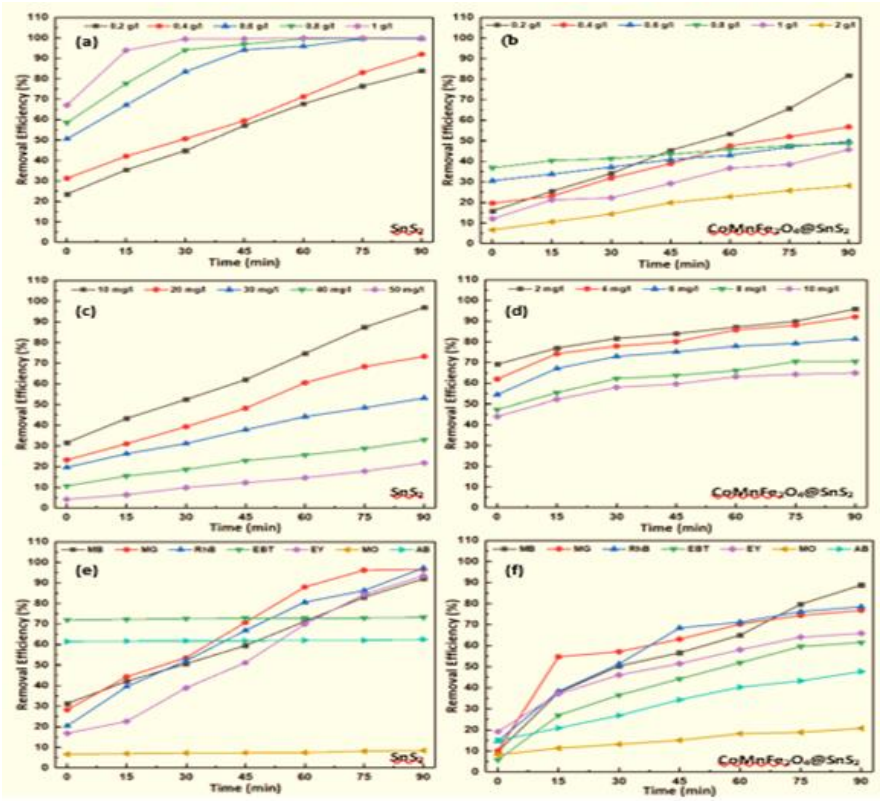

Fig.5. Photocatalytic dye degradation of dyes in presence of (a), (c), (e) SnS2 and (b), (d), (f) CoMnFe2O4@SnS2 under following reaction conditions: (a), (b) varying concentration (0.01 g/l-0.1g/l) of nanomaterial in presence of 10 mg/l MB dye; (c), (d) varying concentration (10 mg/l-50 mg/l) of MB dye in presence of 0.1 g/l of nanomaterial, and (e), (f) in presence of different dyes at 10mg/l concentration and 0.1 g/l of nanomaterial

Discussion

Dye degradation experiments were conducted using MoO_3, MoS_2, SnS_2, and their nanocomposites under visible light. The study explored three experimental setups: varying nanomaterial concentration, varying dye concentration, and testing different dye types. MoO_3 showed the highest degradation efficiency (99% at 0.1 g/L), followed by MoS_2 (80% at 0.6 g/L) and SnS_2 (99% at 0.6 g/L). The nanocomposites demonstrated lower efficiency than their pure counterparts. Kinetic studies confirmed that all six materials followed pseudo-first-order kinetics, ranking MoO_3 as the most effective photocatalyst.

4. Conclusion

MoO_3 nanoparticles emerged as the most efficient photocatalyst for dye degradation under visible light, outperforming MoS_2 and SnS_2. While nanocomposites exhibited some effectiveness, they were less efficient than pure materials. These findings highlight MoO_3 as a promising candidate for wastewater treatment applications.

5. References

[1] WHO (2002). The world health report 2002: Reducing Risks, Promoting Healthy Life. World Health Organization (http://www.who.int/whr/2002/en/whr02_en).

[2] WHO (2012). Progress on Drinking Water and Sanitation: 2012 update. UNICEF and World Health Organization. (https://www.who.int/water_sanitation_health/publications/jmp_report-2012/en/)

[3] Ahmad, A., Mohd-Setapar, S. H., Chuong, C. S., Khatoon, A., Wani, W. A., Kumar, R., & Rafatullah, M. (2015). Recent advances in new generation dye removal technologies: novel search for approaches to reprocess wastewater. RSC Advances, 5(39), 30801-30818.

[4] Akyol, A., & Bayramoglu, M. (2008). The degradation of an azo dye in a batch slurry photocatalytic reactor. Chemical Engineering and Processing: Process Intensification, 47(12), 2150-2156.

[5] Chong, M. N., Jin, B., Chow, C. W., & Saint, C. (2010). Recent developments in photocatalytic water treatment technology: a review. Water research, 44(10), 2997-3027.

[6] Chellam, S., & Cogan, N. G. (2011). Colloidal and bacterial fouling during constant flux microfiltration: Comparison of classical blocking laws with a unified model combining pore blocking and EPS secretion. Journal of Membrane Science, 382(1-2), 148-157.

[7] Chakrabarti, S., & Dutta, B. K. (2004). Photocatalytic degradation of model textile dyes in wastewater using ZnO as semiconductor catalyst. Journal of hazardous materials, 112(3), 269-278.

[8] Grieger, K. D., Hansen, S. F., & Baun, A. (2009). The known unknowns of nanomaterials: describing and characterizing uncertainty within environmental, health and safety risks. Nanotoxicology, 3(3), 222-233.

[9] Gupta, V. K., Kumar, R., Nayak, A., Saleh, T. A., & Barakat, M. A. (2013). Adsorptive removal of dyes from aqueous solution onto carbon nanotubes: a review. Advances in colloid and interface science, 193, 24-34.

[10] Siddiqi, K. S., & Husen, A. (2016). Engineered gold nanoparticles and plant adaptation potential. Nanoscale Research Letters, 11(1), 400.